

Genomic Characterization of a PDX Model of T-DM1-resistant HER2+ Invasive Ductal Carcinoma Using Augmented Exome Sequencing

Elena Helman, PhD, Michael J Wick¹, PhD, Michael J Clark, PhD, Lizette Gamez¹, Sean Boyle, PhD, Kyriakos P. Papadopoulos¹, MD, Shujun Luo, PhD, Anthony W. Tolcher, MD, Mirian Karbelashvili¹, PhD, Parin Sripakdeevong, PhD, Deanna Church, PhD, Christian Haudenschild, PhD, Richard Chen, MD, John West

Contact: elena.helman@personalis.com

¹Personalis, Inc. | Menlo Park, CA // ¹START Inc. | 4383 Medical Dr, San Antonio, TX 78229

Abstract

HER2 amplification/overexpression occurs in 20-30% of breast cancers and is associated with poor prognosis and increased metastatic potential. Patients with HER2+ breast cancers who have progressed on trastuzumab and lapatinib are often prescribed the antibody-drug conjugate, doxorubicin emtansine (T-DM1). Results from the TH3RESA and EMILIA studies showed that T-DM1 increased progression-free and overall survival compared to standard therapy and suggested it be considered as standard of care. Despite these favorable efficacy results, most patients treated with T-DM1 eventually progress, but the mechanisms of resistance are not understood. Acquired resistance to T-DM1 has been shown *in-vitro*, but has not been examined in an *in-vivo* system.

An FNA from a metastatic lung lesion was used to establish a human PDX model from a patient with metastatic HER2+ invasive ductal carcinoma. This model was found resistant to T-DM1 administered weekly at 3 m/kg and every three weeks at 10 m/kg. We performed whole-exome sequencing on both the metastatic tissue and the PDX model using an augmented and content-enhanced exome. The augmented exome is optimized to detect major cancer mutations by enhancing coverage over known sequencing gaps and GC-rich regions across >1300 cancer and 200 miRNA genes. We also performed whole-transcriptome sequencing on the PDX model. All data were analyzed using a cancer bioinformatics pipeline optimized for high-accuracy detection of small variants and indels, somatic copy-number aberrations, gene expression and fusions.

We comprehensively profiled the exomes of a metastatic HER2+ ductal carcinoma resistant to T-DM1 treatment and a PDX model derived from it. We found that the PDX model was highly consistent with the neoplastic tissue, with respect to both somatic variants and copy-number alterations, establishing it as an accurate representation of a patient-derived T-DM1-resistant tumor. We verified only 0.27% contamination by mouse DNA in the PDX model. Specifically, we confirmed the continued amplification of HER2 as well as CCNE1 and MYC. Loss-of-heterozygosity of TP53 was coupled with a clonal damaging point mutation. Of note, we found a non-synonymous mutation in HER2, suggesting possible involvement in resistance mechanisms. Transcriptome data confirmed mutation expression in the RNA and gene expression changes of amplified/deleted genes.

We present the first preclinical model of a human xenograft derived from a HER2+ metastatic breast cancer with acquired T-DM1 resistance. T-DM1 is effective in treating advanced HER2+ breast cancer in patients who have progressed on standard therapies, but this efficacy is short-lived. Here, we used whole-exome and transcriptome sequencing to characterize the genomic profile of tumors that have become resistant to T-DM1 and present a patient-derived model to reveal insights into acquired T-DM1 resistance mechanisms.

Materials and Methods

Tumor Samples and PDX Model

A fine needle aspirate (FNA) from a metastatic lung lesion was used to establish a human PDX model from a Caucasian woman with metastatic HER2+ invasive ductal carcinoma (ER=0%, PR=0%, HER2=3+, Ki67=48%) with acquired resistance to T-DM1 therapy. A sample from a resected metastatic lesion as well as a matched normal from the same patient were also collected prior to T-DM1 resistance (TABLES 1 and 2).

For drug sensitivity studies, tumor fragments from host mice were harvested and implanted subcutaneously into immune-deficient mice; animals were matched by tumor volume (TV) into control and treatment groups and dosing initiated. Tumor volume and animal weight data were collected electronically using a digital caliper and scale; tumor dimensions were converted to volume using the formula: tumor volume (mm³) = width² (mm) x length (mm) x 0.52. Each study was completed once mean group tumor volume reached a predetermined size or a time endpoint was reached; ΔTV of each treated group was compared with control or its starting tumor volume at study endpoint.

Sample Description	Sample Name
Metastatic HER2+ invasive ductal carcinoma sample before T-DM1 resistance	Pre
Metastatic HER2+ invasive ductal carcinoma resistant to T-DM1 treatment	Post
Patient-derived xenograft created from an FNA of the Post sample	PDX
Matched normal	Normal

TABLE 1: Description of samples examined in this analysis and name by which each sample will be referred.

Pre		Post		PDX	
3rd TX PRIOR	2nd TX PRIOR	TX PRIOR	TX PRIOR	2nd TX PRIOR	3rd TX PRIOR
GEMCITABINE	T-DM1	INV-P13-Ki	P13-Ki	CAPE/LAPATINIB	INV-IT AGENT

TABLE 2: Treatment history of the patient with metastatic breast carcinoma. Green triangles represent the time of metastatic tumor resection for Pre and Post samples, respectively.

Pre, Post, PDX and Normal samples were sequenced using an augmented exome platform and tumor samples analyzed through an optimized cancer bioinformatics pipeline using paired tumor and matched normal samples.

Accuracy and Content Enhanced Exome

Many canonical cancer genes, such as TP53, BRAF, and NF1 contain gaps in sequencing coverage through standard NGS. These gaps are often due to high-GC content and low complexity regions. We developed an augmented target enrichment strategy optimized for even coverage across the entire span of gene content. This approach includes multiple nucleic acid enrichments to deal with high-GC content and includes custom oligonucleotides designed to compensate for challenging regions.

FIGURE 1 shows examples of the sequencing coverage produced across several known cancer genes using our approach. Important cancer mutations present in regions of the gene that are poorly covered with standard exomes regain aligned reads and are detected.

In the augmented exome, over 8,000 medically relevant genes are enhanced for even coverage including over 1300 cancer genes.

An optimized cancer bioinformatics pipeline was used to analyze tumor samples in this study. This pipeline was designed to detect SNVs, small InDels, and copy-number alterations at high sensitivity and specificity.

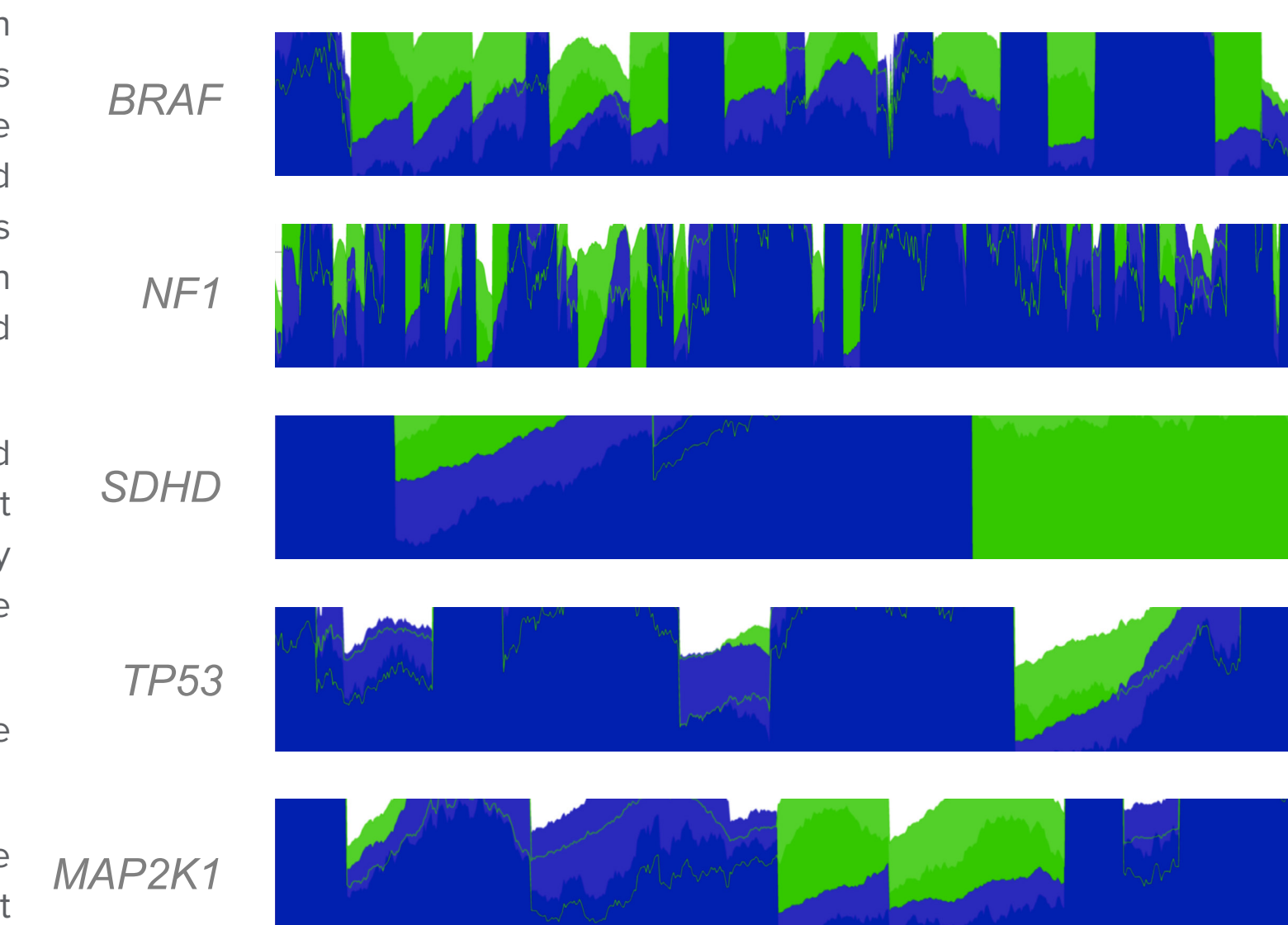


FIGURE 1: Sequencing coverage of select cancer genes with a standard exome (blue) and with our augmented exome (green).

Results

PDX Model Concordance

To determine how accurately the PDX model represents the primary tumor it was derived from, we characterized and compared the exome profile of a primary metastatic tumor sample (Post) with the xenograft model derived from it (PDX). We calculated only 0.27% contamination from the mouse genome in the PDX sequencing data.

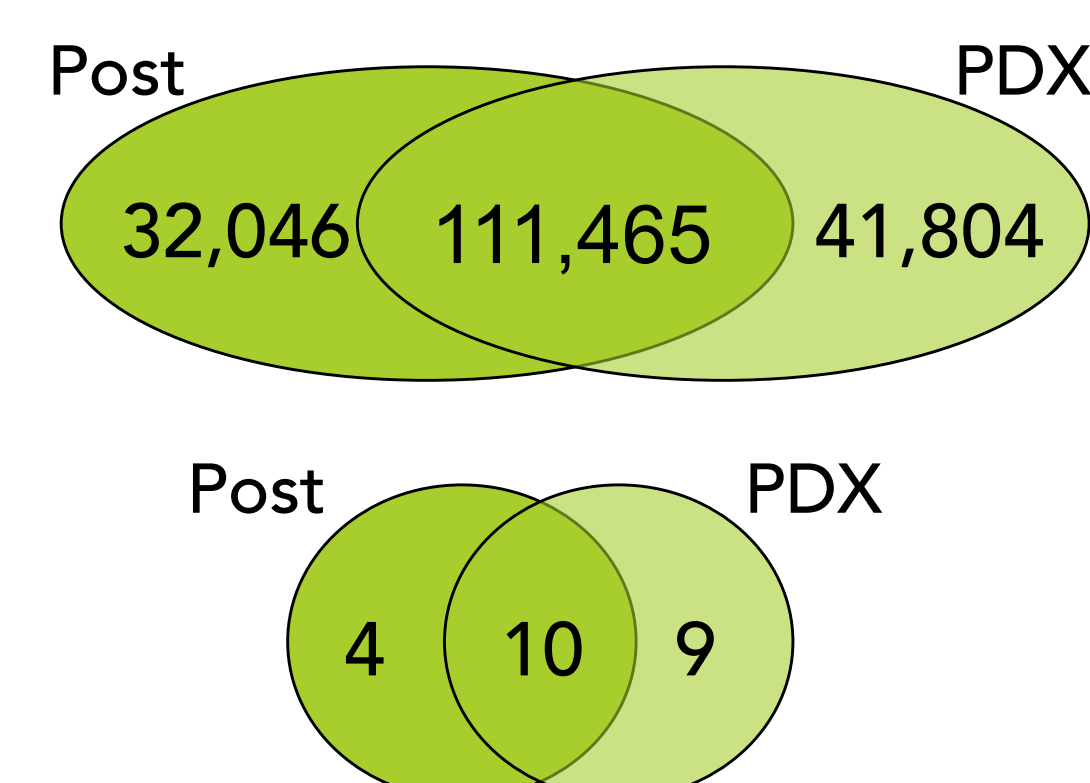
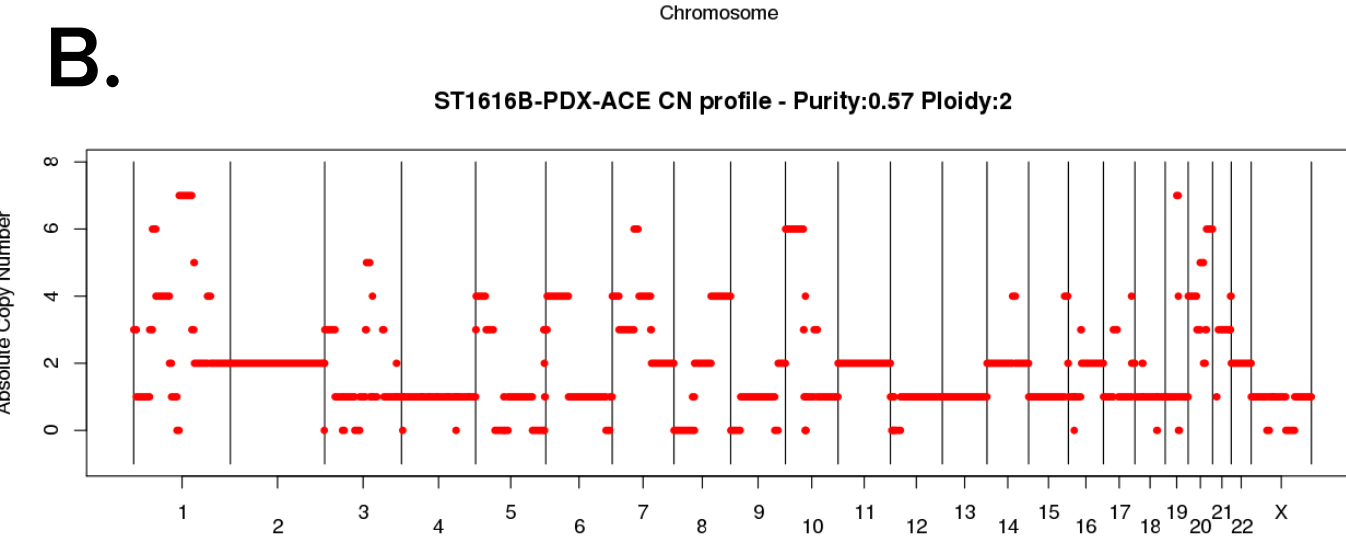
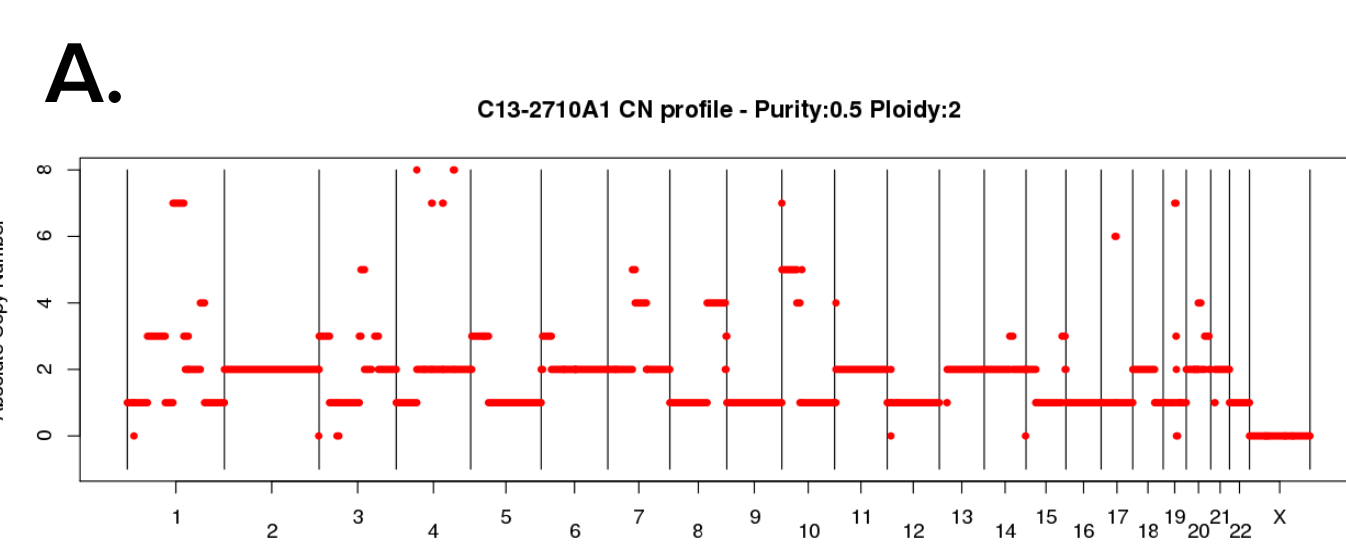


FIGURE 2: All somatic and copy number variants detected in the post-resistance sample (Post) and PDX, top and bottom.

We also assessed the absolute copy number profile of the primary tumor and xenograft model (FIGURE 2). The two profiles are largely similar with focal amplifications of chromosomes 17, amplification of chr10p, a one-copy deletion of chromosomes 12, 15 and 17. However, it is clear that the PDX acquired some novel copy-number aberrations during engraftment and further.

Mouse Contamination 0.27%

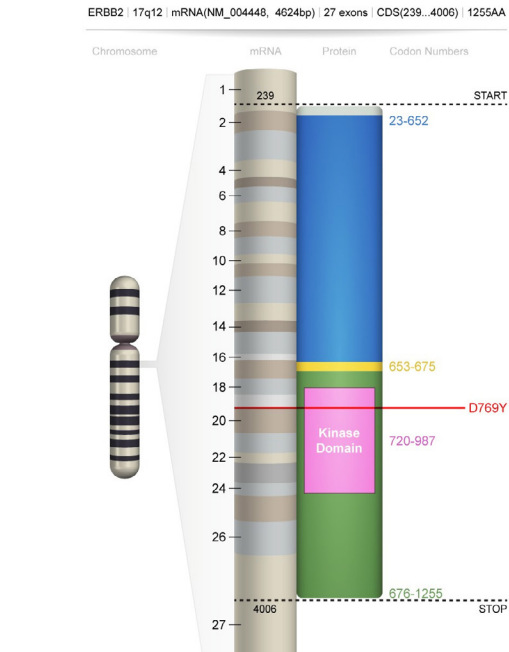
Small variants – point mutations and short insertions/deletions – were compared between the Post and PDX samples (FIGURE 3). We observe high concordance between all variants called in each sample (FIGURE 3A). Variants detected in the PDX sample, alone, tended to be lower allele frequency, representing further tumor evolution in the host or



FIGURES 3A and 3B: Absolute copy number profile of primary Post tumor sample (A) and the PDX model derived from it (B).

ERBB2 D769Y

We discover a high-frequency missense mutation in the kinase domain of ERBB2, D769Y, in all tumor samples assessed. This somatic mutation has previously been detected in <1% of cancers amongst large studies (FIGURE 4).



ERBB2 is currently clinically actionable when amplified or overexpressed, but studies of clinical genetic profiling of tumors found >40% of ERBB2 alterations were point mutations², including 3 breast carcinomas reported with ERBB2 D769Y. Recent studies have identified this mutation as activating and likely driving tumorigenesis in HER2 negative breast cancers³.

Cells with this mutation display an invasive morphology that was inhibited by lapatinib and trastuzumab, *in vitro*³. Studies on this mutation to date, however, have focused on a HER2 negative background.

FIGURE 4: Diagram of ERBB2 protein domains with the D769Y mutation highlighted in red.

Small Variants

We characterized the genomic profiles of a metastatic HER2+ ductal carcinoma before acquired resistance to T-DM1 therapy and a sample taken after resistance. Several mutations in canonical cancer genes are consistently detected at high allelic fractions (TABLE 4). The PDX model often has higher allelic fractions due to higher tumor purity as well as acquired loss of heterozygosity in some regions.

Gene	Mutation	Pre	Post	PDX
TP53	L184R	0.48	0.38	0.99
ERBB2	D769H	0.80	0.75	0.91
BIRC5	G52E	0.22	0.21	0.36
DCAF5	E771*	0.22	0.42	0.48

TABLE 4: Select somatic variants in high-impact cancer genes, columns Pre, Post, and PDX detail the variant allelic frequency in each sample accordingly.

Copy Number

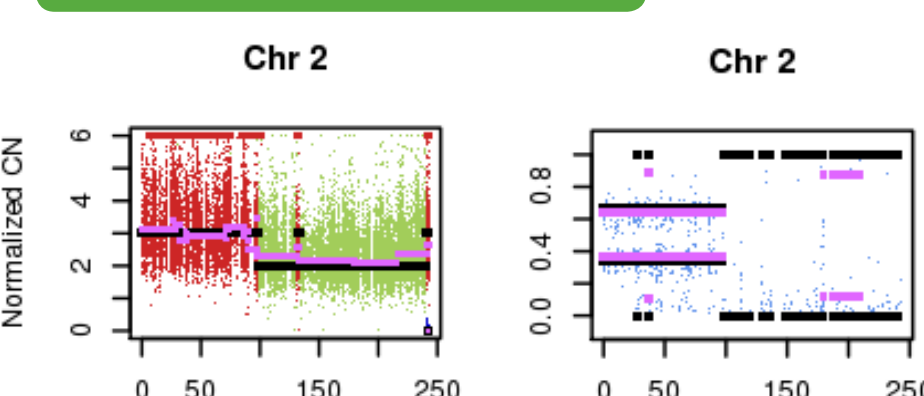


FIGURE 6: Copy number ratio of tumor/normal read depth across chromosome 2 (left). Green represents normal copy number of 2 whereas red depicts an amplification to copy number 3. Right, B-allele frequency (BAF) plot across chr2.

COSMIC	CBIO	MD Anderson	Clinical Tumor Profiling
4 / 10061 (<1%)	4 / 19645 (<1%)	1 / 2747 (<1%)	3 / 2221 (1.35%) ²

TABLE 3: Diagram of ERBB2 protein domains with the D769Y mutation highlighted in red. B: Table of mutation occurrence across large cancer studies¹.

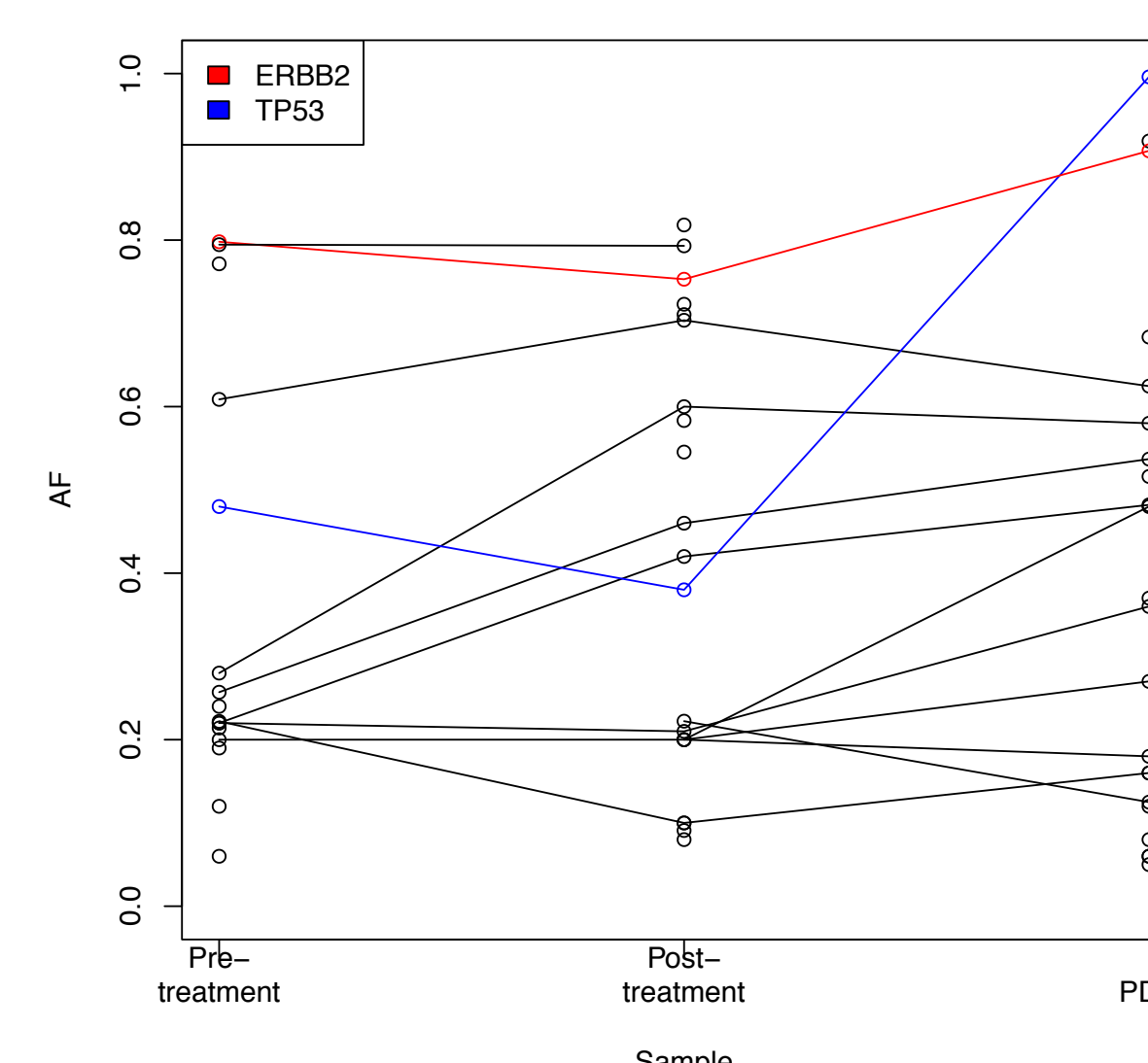


FIGURE 5: Allele frequency (AF) of somatic cancer variants in each of the three tumor samples examined here (Pre, Post, and PDX).

HER2 amplification occurs in 18-20% of breast cancers and has been shown to confer increased sensitivity to targeted agents, such as trastuzumab. We observe HER2 (ERBB2) genomic amplification in each of the specimens analyzed. Using read-depth as well as minor-allele frequency information from the exome data, we are also able to detect amplifications/deletions of other genes involved in cancer.

Interestingly, the sample resected before resistance exhibits more gene amplifications and deletions than do the Post/PDX samples. Hyperamplification of certain oncogenes associated with breast cancer, such as CCNE1 and NOTCH2, is consistent across all three samples (FIGURE 7).

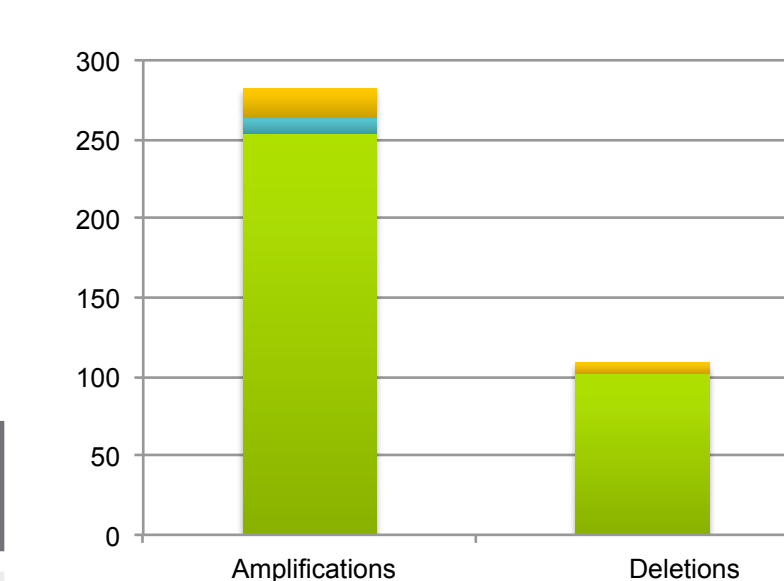


FIGURE 7: Number of gene amplifications/deletions detected in each of the samples.

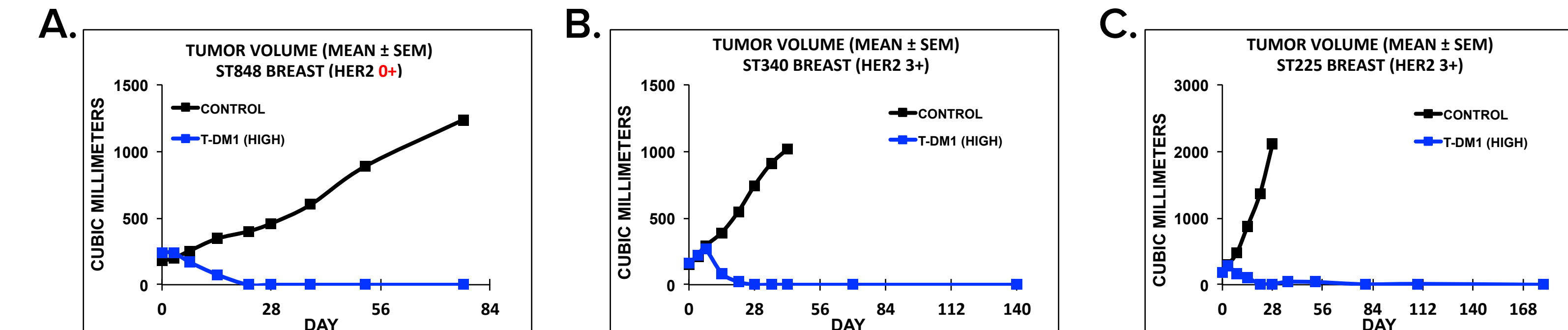
Gene	Pre	Post	PDX
ERBB2	44	10	21
PIK3CB/MRAS/FOXO2	128	21	36
NOTCH2	49	10	12
CCNE1	17	11	17

TABLE 5: Select gene amplifications and the copy number detected in each sample.

References

- Personalized Cancer Therapy – Knowledge Base for Precision Medicine. MD Anderson Cancer Center. <https://pct.mdanderson.org/genes/alteration?geneName=ERBB2&alterationName=D769Y>
- Frampton et al. Development and validation of a clinical cancer genomic profiling test based on massively parallel DNA sequencing. Nature Biotech (2012).
- Bose et al. Activating HER2 mutations in HER2 gene amplification negative breast cancer. Cancer Discovery (2013).

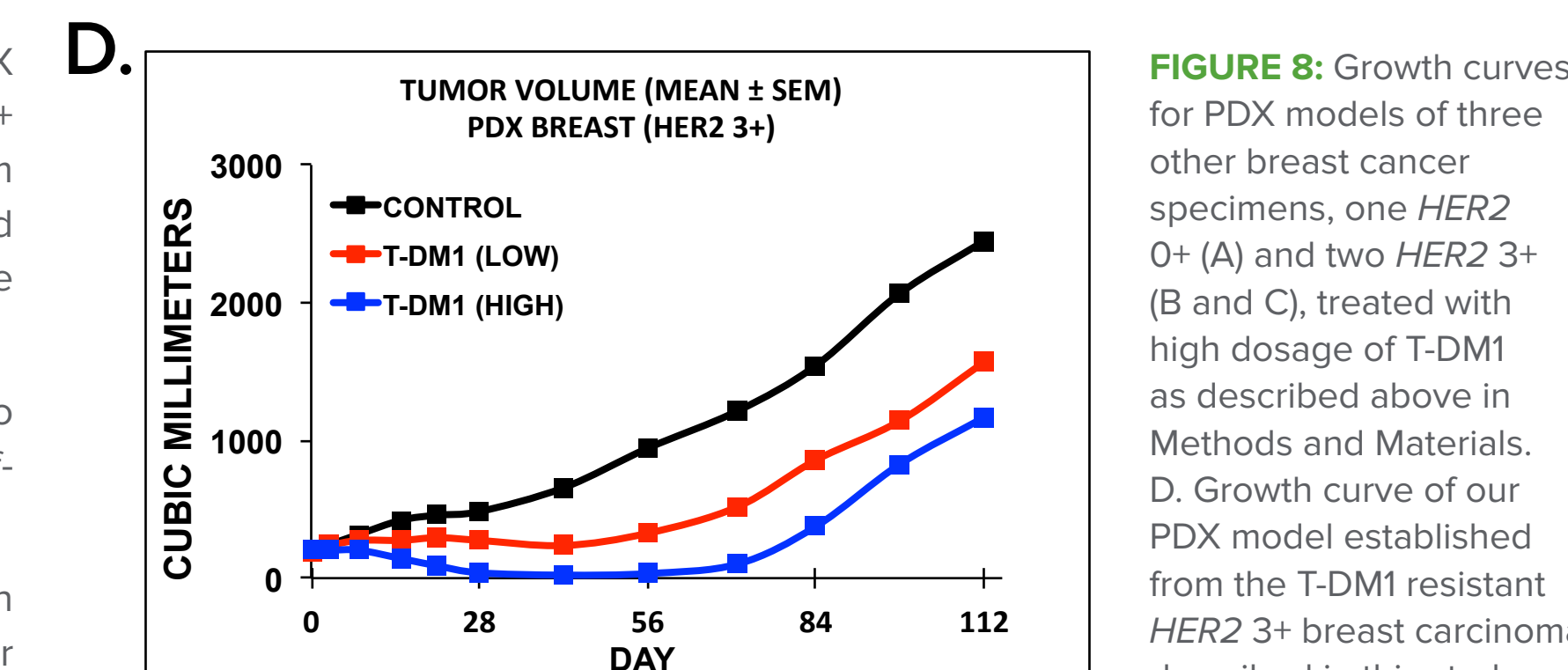
PDX Model Resistance to T-DM1



We measured sensitivity to T-DM1 treatment *in vitro* for our PDX model as well as three other PDX models derived from two HER2+ and one HER2- breast carcinomas, respectively, established from trastuzumab refractory patients. The PDX model demonstrated reduced sensitivity to T-DM1 treatment compared with these other HER2 3+ models (FIGURE 8).

Interestingly, the HER2=0+ model ST848 was very sensitive to T-DM1 even without target expression suggesting some off-target effects or an alternative mechanism for sensitivity.

The PDX model showed initial sensitivity to both low and high doses of T-DM1 by 36 days, but then acquired resistance after 56 days. Thus, the PDX model appears to recapitulate the phenotype of drug resistance exhibited by the patient.



Sensitivity to Targeted Agents

HER2 amplification is a major therapeutic target in breast cancer and is often targeted by FDA-approved, HER2-targeted drugs, trastuzumab, pertuzumab, and lapatinib. Additional HER2-targeted drugs currently undergoing clinical trials include neratinib, an irreversible HER2/EGFR tyrosine kinase inhibitor, and T-DM1.

The rare somatic mutation, HER2 D769Y, has recently been shown to be an activating mutation in HER2 negative breast cancer models³. This mutation has also been shown to confer sensitivity to neratinib³. It has been postulated that the D769Y/H/Y mutations may increase hydrophobic contacts and thereby increase HER2 dimerization.

We tested our PDX model for sensitivity against six HER2 targeted agents (FIGURE XX). Test agents were formulated in appropriate vehicles and administered via oral (neratinib, capecitabine, lapatinib), intraperitoneal (trastuzumab, pertuzumab) or intravenous (T-DM1) injection. All agents were clinically sourced except research-grade neratinib (LC Labs).

We find that that our model of a HER2+ breast carcinoma with a D769Y HER2 mutation also displays sensitivity to neratinib alone, consistent with previous literature.

Conclusions

T-DM1 is effective in treating advanced HER2+ breast cancer in patients who have progressed on standard therapies, but this efficacy is short-lived. Here, we used whole-exome and transcriptome sequencing to characterize the genomic profile of tumors that have become resistant to T-DM1 and present a patient-derived model to reveal insights into acquired T-DM1 resistance mechanisms.



AACR 2015 | Booth 2156

Personalis®

Pioneering Genome-Guided Medicine